Journal of the Ceramic Society of Japan 116 [12] 1314-1318 2008 **Paper**

Crystal growth behavior in CuO-doped lithium disilicate glasses by continuous-wave fiber laser irradiation

Tsuyoshi HONMA,† Phan Thao NGUYEN and Takayuki KOMATSU

Department of Materials Science and Technology, Nagaoka Univerisity of Technology, 1603−1, Kamitomioka, Nagaoka 940−2188

Crystal growth behaviors in CuO-doped Li_2O–$2SiO_2$ glasses by continuous-wave (cw) Ytterbium doped fiber laser (wavelength: 1080 nm) irradiations are examined. The lines (width: ~5 μm) consisting of highly oriented nonlinear optical lithium disilicate ($Li_2Si_2O_5$) crystals are patterned in various laser powers (1.2–2.4 W) and scanning speeds (2–42 μm/s), and it is found that the crystal growth having the rates of 1 to 32 μm/s gives crystal lines with smooth surface morphologies. The critical (maximum) growth rates of $Li_2Si_2O_5$ crystals in cw fiber laser irradiations are compared with the crystal growth kinetics (the reference data) in the Li_2O–$2SiO_2$ glass system determined by a conventional crystallization method in electric furnaces. It is proposed that the temperature of the fiber laser irradiated region for the $Li_2Si_2O_5$ crystal growth would be 650–850°C. It is of importance to avoid crystal nucleation during laser irradiations for the patterning of homogeneous crystal lines.

Key-words : Lithium disilicate glass, Laser irradiation, Crystallization, Growth rate, Second harmonic generation

[Received September 30, 2008; Accepted November 20, 2008]

1. Introduction

Crystallization of glass caused by laser irradiations has been regarded as a process for spatially selected crystallization in glass. The present authors' group[1)–9)] proposed two laser irradiation techniques for the patterning of crystal dots and lines at the glass surface, i.e., rare-earth atom heat (REAH) processing and transition metal atom heat (TMAH) processing, in which conventional lasers such as continuous-wave (cw) lasers with a near infrared wavelength (λ = 1064 nm) have been used for glasses containing rare-earth (RE) ions such as Sm^{3+} and Dy^{3+} and transition metal (TM) ions such as Ni^{2+} and Cu^{2+}. Using these techniques, the present authors' group has succeeded in patterning crystal lines consisting of nonlinear or ferroelectric crystals such as β-BaB_2O_4, β'-$Sm_2(MoO_4)_3$, $Ba_2TiGe_2O_8$, $Ba_2TiSi_2O_8$, (Sr,Ba)Nb_2O_6, and $LiNbO_3$. In the writing of uniform and oriented crystal lines in glasses, it is of important to understand the relationship between laser irradiation conditions (laser power, scanning speed, etc) and crystal growth rates. In other words, it would be of importance to estimate the temperature of laser-irradiated spots.

In the present study, we report crystal growth behaviors in CuO-doped Li_2O–$2SiO_2$ glasses by laser irradiations, in which cw Ytterbium doped fiber lasers with λ = 1080 nm are used and lines consisting of lithium disilicate ($Li_2Si_2O_5$) crystals are patterned. The crystal structure of $Li_2Si_2O_5$ is orthorhombic (a = 0.5807 nm, b = 1.4582 nm, c = 0.4773 nm) with a space group of noncentrosymmetric $Ccc2$.[10)] The composition of base glass Li_2O–$2SiO_2$ corresponds to that of the $Li_2Si_2O_5$ crystalline phase, and CuO is added as absorbent for irradiated lasers. Many studies on the crystallization behaviors in Li_2O–$2SiO_2$ glasses have been reported so far, and nucleation and crystal growth rates of $Li_2Si_2O_5$ crystals in the crystallization in electric furnaces have been clarified as a function of heat treatment temperature.[11)–17)] Furthermore, it should be pointed out that $Li_2Si_2O_5$ is the second-order nonlinear optical crystalline phase.[18),19)] It is, therefore, of interest to pattern $Li_2Si_2O_5$ crystal lines by laser irradiations and to clarify crystal growth behaviors in the laser-induced crystallization for Li_2O–$2SiO_2$ glasses.

2. Experimental procedure

The compositions of the glasses examined in this study are xCuO·33.3Li_2O·66.7SiO_2 with x = 0, 1, and 2 (in the molar ratio). The glasses were prepared by a conventional melt quenching method. Commercial powders of reagent grade Li_2CO_3, SiO_2, and CuO were mixed together and melted in a platinum crucible at 1300°C for 40 min in an electric furnace. The melts were poured onto an iron plate and pressed to a thickness of ~1.5 mm by another iron plate. The values of the glass transition T_g and crystallization peak T_p temperatures were determined using differential thermal analyses (DTA) at a heating rate of 10 Kmin^{-1}. The quenched glasses were annealed around T_g to release internal stresses, and then polished mechanically to get a mirror finish with CeO_2 powders. Before laser irradiations, the glasses were heat-treated at various temperatures in an electric furnace and usual crystallization behaviors were examined. The crystalline phases formed by heat treatments were identified by X-ray diffraction (XRD) measurements.

The polished surface of the glasses was irradiated with cw Ytterbium doped fiber lasers with λ = 1080 nm. The laser beam was focused on the surface of the glasses using an objective lens (magnification of 50, numerical aperture (NA) of 0.81), and the sample stage was automatically moved during laser irradiations to construct line patterns. Crystal lines patterned by laser irradiations were observed with a polarization optical microscope. Polarized micro-Raman-scattering spectra at room temperature for the crystal lines patterned by laser irradiations were measured with a laser microscope (Tokyo Instruments Co. Nanofinder) operated at Ar^+ laser (λ = 488 nm). Second harmonic (SH) intensities arising from crystal lines were measured by using a fundamental wave of Q-switched Nd:YAG laser with λ = 1064

† Corresponding author: T. Honma; E-mail: honma@mst.nagaokaut.ac.jp

nm as an incident laser source, in which linearly polarized fundamental laser lights were introduced into crystal lines, and SH intensities were measured as a function of the angle between crystal lines and linearly polarized lasers (i.e., the azimuthal dependence of SH signals).

3. Results and discussion

3.1. Crystallization in electric furnace

The values of T_g and T_p for the glasses prepared in this study are listed in **Table 1**, giving the values of T_g = 462 and T_p = 653°C for $33.3Li_2O{\cdot}66.7SiO_2$ glass (designated here as the base glass), T_g = 454 and T_p = 651°C for $1CuO{\cdot}33.3Li_2O{\cdot}66.7SiO_2$ glass (designated here as 1CuO-doped glass), and T_g = 450 and T_p = 586°C for $2CuO{\cdot}33.3Li_2O{\cdot}66.7SiO_2$ glass (designated here as 2CuO-doped glass). It is seen that the addition of CuO tends to decrease the glass transition and crystallization temperatures. All the melt-quenched samples showed optically transparencies. The optical absorption spectra at room temperature for the CuO-doped glasses were measured in the wavelength range of 250–2000 nm using a spectrometer (Shimadzu UV–3150). A broad and asymmetrical peak centered at ~800 nm was observed. It is known that Cu^{2+} ions with the electronic configuration of $3d^9$ in oxide glasses give a strong and broad absorption peak at around 800 nm, and this peak is assigned to the $^2B_{1g}\rightarrow{}^2B_{2g}$ transition in Cu^{2+} ions in octahedral sites with strong tetragonal distortions.[20),21)] The optical absorption coefficients, α, at 1080 nm for the CuO-doped glasses are also shown in Table 1. The values of α = 4.1 and 8.3 cm^{-1} for Cu^{2+} ions would be enough for crystallizations of CuO-doped $Li_2O–2SiO_2$ glasses with T_p = 586 and 651°C when using our experimental setup.[5),9)]

Table 1. Values of Glass Transition Temperature T_g, Crystallization Peak Temperature T_x, and Optical Absorption Coefficient α at 1080 nm for xCuO·33.3Li_2O·66.7SiO_2 (x = 0, 1, and 2) Glasses

Glass	T_g (°C)	T_p (°C)	α (cm^{-1})
x = 0	462	653	–
x = 1	454	651	4.1
x = 2	450	586	8.3

The powder XRD patterns for the crystallized samples obtained by heat treatments at T_p for 3 h in air are shown in **Fig. 1**. All the peaks appeared are assigned to the stable lithium disilicate $Li_2Si_2O_5$ crystalline phase with an orthorhombic structure (ICDD: 17–447). It is known that a metastable lithium metasilicate Li_2SiO_3 crystalline phase is formed in the early crystallization of $Li_2O–2SiO_2$ glasses.[13),16)] As can be seen in Fig. 1, however, the formation of Li_2SiO_3 crystals was not detected. Although the shape of XRD patterns in heat-treated samples differed from reference data in each other, it may originate from grain size of specimen. The XRD patterns for the surface of the crystallized samples heat-treated at T_p for 3 h are shown in **Fig. 2**. The diffraction peaks with strong intensities corresponding to the (002) plane in $Li_2Si_2O_5$ crystals are observed at the angle of around 2θ = 37°, indicating that $Li_2Si_2O_5$ crystals are oriented at the surface, i.e., the c-axis orientation. The results shown in Figs. 1 and 2 indicate that CuO-doped $Li_2O–2SiO_2$ glasses show almost similar crystallization behaviors in spite of the addition (1 and 2 mol) of CuO. Ding et al.[18)] reported that $Li_2O–2SiO_2$ glasses exhibit the surface crystallization giving the c-axis orientation of $Li_2Si_2O_5$ crystals. Engel and Frischat[12)] fabricated textured lithium disilicate glass-ceramics with highly oriented $Li_2Si_2O_5$ crystals by moving the glass ($Li_2O–2SiO_2$) through a temperature gradient. As a common feature, therefore, it should be pointed out that $Li_2O–2SiO_2$ glasses show a prominent surface crystallization giving a c-axis orientation of $Li_2Si_2O_5$ crystals.

3.2. Laser-induced crystallization

The fiber lasers with λ = 1080 nm were irradiated onto the surface of 1CuO-doped glass, in which the laser power P was 2.1–2.3 W and the laser scanning speed S was 2–32 μm/s. The

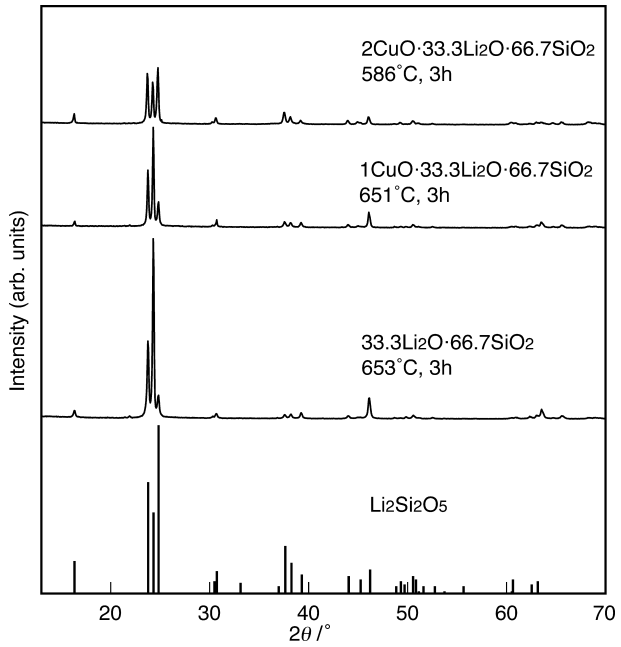

Fig. 1. Powder XRD patterns at room temperature for the crystallized samples obtained by heat treatments at T_p for 3 h in xCuO·33.3Li_2O·66.7SiO_2 (x = 0, 1, 2) glasses.

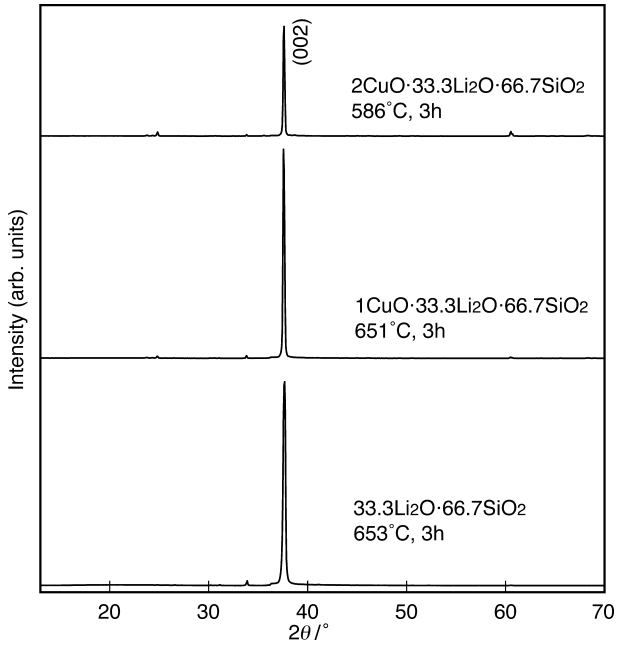

Fig. 2. XRD patterns at room temperature for the surface of the crystallized samples heat-treated at T_p for 3 h in xCuO·33.3Li_2O·66.7SiO_2 (x = 0, 1, 2) glasses.

polarized optical micrographs for the samples obtained by laser irradiations are shown in **Figs. 3** to **5**. The morphological changes with a width of ~5 μm are clearly observed. Except the line patterned by the laser irradiations with P = 2.3 W and S = 2 μm/s in Fig. 5, each line shows a homogeneous color's distribution along the scanning direction, indicating that a stable structural change is taking place under a given laser irradiation condition.

The polarized micro-Raman scattering spectra at room temperature for the line patterned by the laser irradiations with P = 2.1 W and S = 9 μm/s in 1CuO-doped glass are shown in **Fig. 6**. In the measurements, the direction of Z-axis in the configurations corresponds to the line growth direction, i.e., the laser scanning direction. For instance, the configuration of $y(zz)\bar{y}$ means that incident laser introduced from Y-axis direction has a polarization (electric vector) of Z-axis and Raman light with polarization of

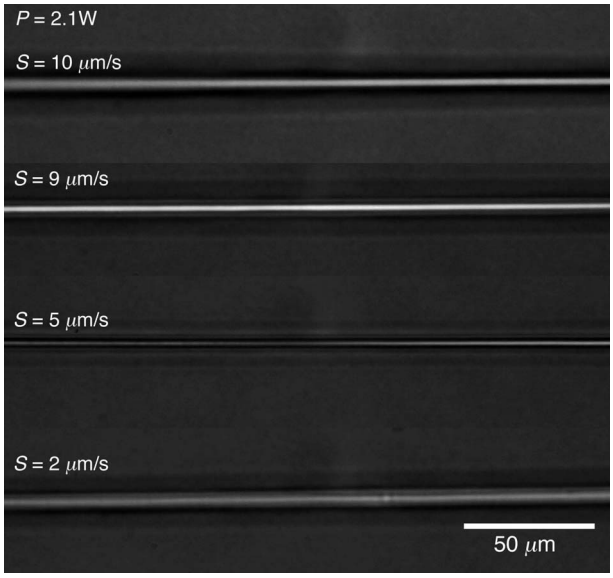

Fig. 3. Polarized optical micrographs for the samples obtained by laser irradiations in 1CuO·33.3Li_2O·66.7SiO_2 glass. The laser power is P = 2.1 W and laser scanning speeds are S = 2, 5, 9, and 10 μm/s.

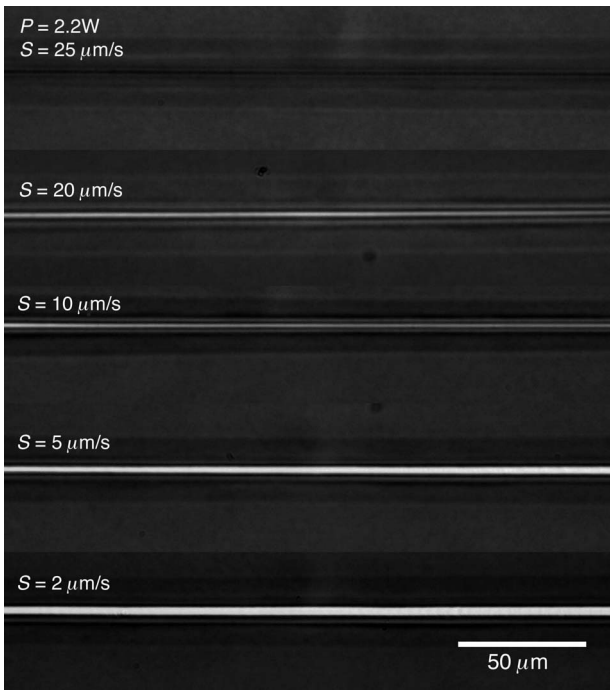

Fig. 4. Polarized optical micrographs for the samples obtained by laser irradiations in 1CuO·33.3Li_2O·66.7SiO_2 glass. The laser power is P = 2.2 W and laser scanning speeds are S = 2, 5, 10, 20, and 25 μm/s.

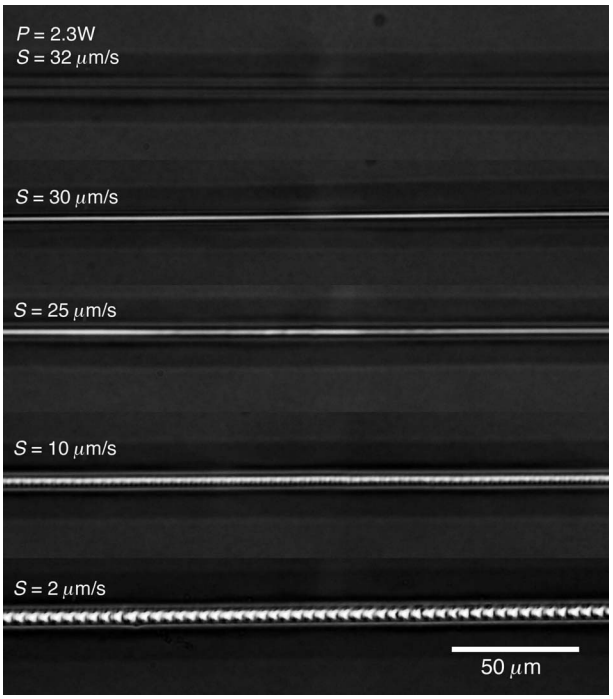

Fig. 5. Polarized optical micrographs for the samples obtained by laser irradiations in 1CuO·33.3Li_2O·66.7SiO_2 glass. The laser power is P = 2.3 W and laser scanning speeds are S = 2, 10, 25, 30, and 32 μm/s.

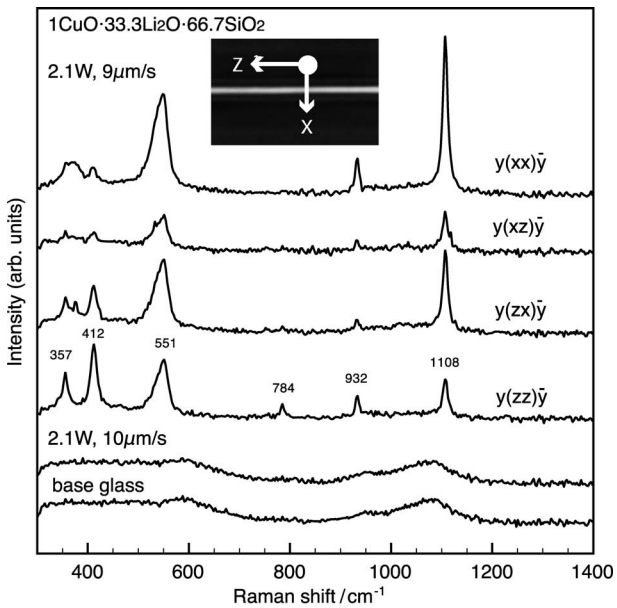

Fig. 6. Polarized micro-Raman scattering spectra at room temperature for the line patterned by laser irradiations with P = 2.1 W and S = 9 and 10 μm/s in 1CuO·33.3Li_2O·66.7SiO_2 glass. The spectrum for the glass part is also included.

Z-axis is detected from $-Y$ direction (backscattering arrangement). As can be seen in Fig. 6, several sharp peaks are observed at 357, 412, 551, 784, 932, and 1108 cm^{-1}. Comparing these spectra with the Raman scattering spectrum for the surface crystallized sample with *c*-axis oriented $Li_2Si_2O_5$ crystals, the peaks shown in Fig. 6 are assigned to the $Li_2Si_2O_5$ crystalline phase. That is, the laser irradiations with P = 2.1 W and S = 9 μm/s onto the surface of 1CuO-doped glass induce the crystallization and the line patterned consists of $Li_2Si_2O_5$ crystals. The relative peak intensities among the Raman bands change largely depending on the configuration, suggesting that $Li_2Si_2O_5$ crystals in the crystal line might be oriented.

The azimuthal dependence of the SH intensity for the line patterned by the laser irradiations with P = 2.1 W and S = 9 μm/s in 1CuO-doped glass is shown in **Fig. 7**, in which the measurements were carried out in two configurations of V–V and V–H. In the V–V mode, the polarization of incident lasers is parallel to the polarization of SH waves in the observation, and the V–H mode means the cross-nicol relation. Since clear second harmonic generations (SHGs) were detected, $Li_2Si_2O_5$ crystals formed in the line are nonlinear optical crystals. It is seen that the SH intensity pattern depends on the configuration. In particular, in the V–V mode, the maximum SH intensities are observed at the rotation angles of 0° and 180°. These profiles represent the two-fold angular dependence in the rotation and indicate the orientation of $Li_2Si_2O_5$ crystals in the line patterned by the laser irradiations with P = 2.1 W and S = 9 μm/s.

3.3. Crystal growth rate in laser-induced crystallization

The micro-Raman scattering spectrum for the line patterned by the laser irradiations with P = 2.1 W and S = 10 μm/s for 1CuO-doped glass is shown in Fig. 6. No sharp peak was observed in the spectrum, and the shape of the spectrum is almost the same as that for the base glass as shown in Fig. 6. It is, therefore, concluded that the laser irradiation condition of P = 2.1 W and S = 10 μm/s induces just only the structural modification giving the refractive index change, but not any crystallizations. It was also clarified from micro-Raman spectrum measurements that the lines patterned by the laser irradiations with P = 2.1 W and S = 2 and 5 μm/s consist of $Li_2Si_2O_5$ crystals. From these results, in the laser irradiations at the fixed power of P = 2.1 W for 1CuO-doped glass, the formation of $Li_2Si_2O_5$ crystals, i.e., the patterning of homogeneous crystal lines, is induced at least under the scanning speeds of less than S = 9 μm/s. In other words, the critical crystal growth rate $U_{crystal}$ for $Li_2Si_2O_5$ crystals at the laser irradiations with P = 2.1 W in $1CuO{\cdot}33.3Li_2O{\cdot}66.7SiO_2$ glass is considered to be close to the value of 9 μm/s, i.e., $U_{crystal}$ = 9 μm/s.

For $1CuO{\cdot}33.3Li_2O{\cdot}66.7SiO_2$ and $2CuO{\cdot}33.3Li_2O{\cdot}66.7SiO_2$ glass, laser irradiation experiments at various laser powers and scanning speeds were carried out, and the formation of $Li_2Si_2O_5$ crystals was examined from micro-Raman scattering spectrum measurements. The values of $U_{crystal}$ determined from these experiments are summarized in **Fig. 8**. For 2CuO-doped glass, $Li_2Si_2O_5$ crystals are induced by small laser powers compared with 1CuO-doped glass. It is considered that the temperature of the laser-irradiated region increases with increasing Cu^{2+} content and laser powers, and thus the results shown in Fig. 8 would be reasonable. It should be pointed out that plate-shape glass samples were fractured under the laser irradiation conditions with the scanning speeds of over S = 50 μm/s. Since the laser irradiation gives a rapid heating and rapid cooling, plate-shape glasses would be fractured due to laser-induced thermal stresses. The values of $U_{crystal}$ in the present study are, therefore, ranging from 1 to 40 μm/s.

Burger and Weinberg[14] summarized the data of the isothermal crystal growth rates of $Li_2Si_2O_5$ at various temperatures in Li_2O–$2SiO_2$ glasses reported by many researchers. We reproduced the data summarized by them in **Fig. 9** in this paper and marked the values of $U_{crystal}$ = 1–40 μm/s obtained in the present study with a solid line circle. It is seen that the values of $U_{crystal}$ = 1–40 μm/s correspond to the isothermal crystal growth rates at the temperature range of 650–850°C. It is noted that these temperatures are considerably high compared with the values of the glass transition (T_g = 450–454°C) and crystallization peak (T_p = 586–651°C) temperatures in the CuO-doped $33.3Li_2O{\cdot}63.7SiO_2$ glasses

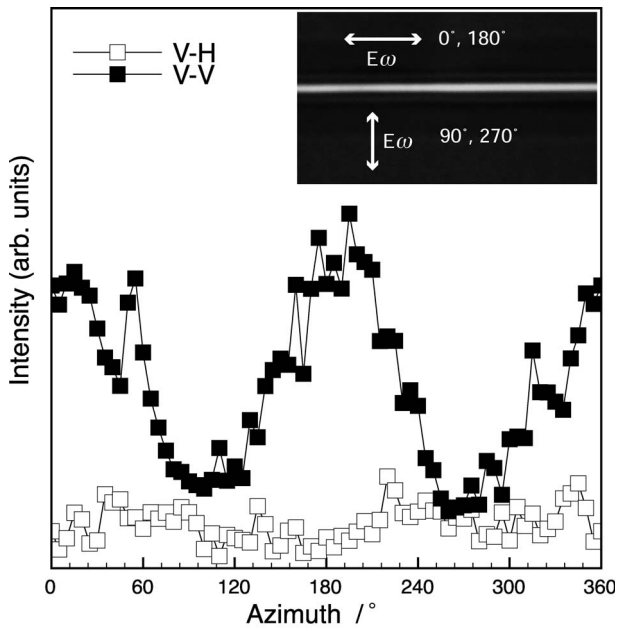

Fig. 7. Azimuthal dependences of the SH intensity for the line patterned by the laser irradiations with P = 2.1 W and S = 9 μm/s in $1CuO{\cdot}33.3Li_2O{\cdot}66.7SiO_2$ glass. The configuration of polarization of fundamental wave ($E\omega$) and line was also shown.

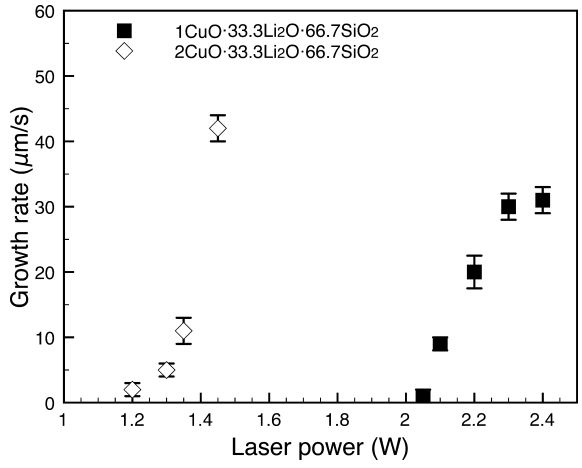

Fig. 8. Critical crystal growth rates at different laser powers determined from laser irradiation experiments xCuO·33.3Li2O·66.7SiO2 glasses (x = 1 and 2).

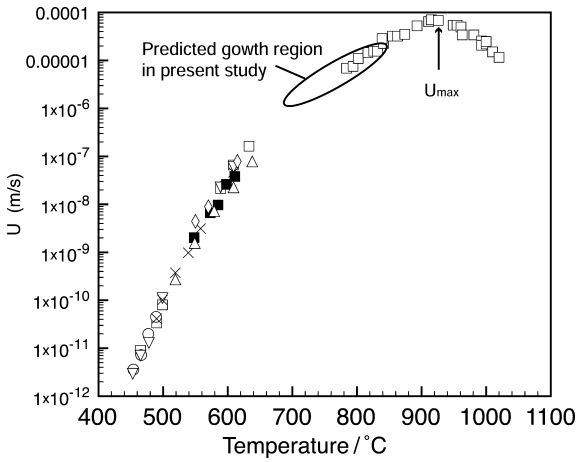

Fig. 9. Growth rates of $Li_2Si_2O_5$ crystals at different heat treatment temperatures in usual crystallizations in electric furnaces for Li_2O–$2SiO_2$ glasses summarized by Burger and Weinberg.[13] The critical crystal growth rates of $U_{crystal}$ = 1–40 μm/s determined in the present study is marked by a solid line circle.

examined in this study. It is expected that in such high temperatures of 650–850°C nucleation rates of $Li_2Si_2O_5$ crystals would be small. Furthermore, as seen in Fig. 9, the values of $U_{crystal}$ = 1–40 μm/s are located at the side being close to the maximum isothermal crystal growth rate U_{max}. This might be one reason for the successful patterning of homogeneous crystal lines consisting of oriented $Li_2Si_2O_5$ crystals in the laser irradiations for CuO-doped $33.3Li_2O{\cdot}66.7SiO_2$ glasses. As indicated in Fig. 2, xCuO·$33.3Li_2O{\cdot}66.7SiO_2$ glasses (x = 0, 1 and 2) show prominent surface crystallizations giving a c-axis orientation of $Li_2Si_2O_5$ crystals at the surface. This kind of prominent surface crystallizations would be also an important point for the homogeneous crystal line pattering in lithium disilicate glasses.

4. Conclusion

The glasses of xCuO·$33.3Li_2O{\cdot}66.7SiO_2$ (x = 0, 1, and 2) were prepared using a conventional melt quenching technique, and cw fiber lasers with λ =1080 nm were irradiated onto the glass surface. The lines consisting of $Li_2Si_2O_5$ crystals were patterned under various laser irradiation conditions, and it was found that $Li_2Si_2O_5$ crystals in the lines are oriented and exhibit SHGs. The critical (maximum) crystal growth rates in the laser irradiations were estimated to be 1 to 32 μm/s, and these values were found to correspond to the isothermal crystal growth rates at 650–850°C in usual crystallizations of Li_2O–$2SiO_2$ glasses in electric furnaces. It is of importance to avoid crystal nucleation during laser irradiations for the patterning of homogeneous crystal lines.

Acknowledgments This work was supported from the Grant-in-Aid for Scientific Research from the Ministry of Education, Science, Sports, Culture and Technology, Japan.

References

1) R. Sato, Y. Benino, T. Fujiwara and T. Komatsu, *J. Non-Cryst. Solids*, **289**, 228–230 (2001).
2) T. Honma, Y. Benino, T. Fujiwara, R. Sato and T. Komatsu, *J. Ceram. Soc. Japan*, **110**, 398–402 (2002).
3) T. Honma, Y. Benino, T. Fujiwara, T. Komatsu and R. Sato, *Appl. Phys. Lett.*, **83**, 2796–2798 (2003).
4) R. Ihara, T. Honma, Y. Benino, T. Fujiwara, R. Sato and T. Komatsu, *Solid State Commun.*,**136**, 273–277 (2005).
5) T. Honma, Y. Benino, T. Fujiwara and T. Komatsu, *Appl. Phys. Lett.*, **88**, 231105 (2006).
6) T. Komatsu, R. Ihara, T. Honma, Y. Benino, R. Sato, H. G. Kim and T. Fujiwara, *J. Am. Ceram. Soc.*, **90**, 699–705 (2007).
7) R. Nakajima, T. Honma, Y. BEnino and T. Komatsu, *J. Ceram. Soc. Japan*, **115**, 582–587 (2007).
8) P. Gupta, H. Jain, D. B. Williams, T. Honma, Y. Benino and T. Komatsu, *J. Am. Ceram. Soc.*, **91**, 110–114 (2008).
9) T. Honma, Y. Benino and T. Komatsu, *J. Mater. Res.*, **23**, 885–888 (2008).
10) B. H. W. S. de Jong, P. G. G. Slaats, H. T. J. Supèr, N. Veldman and A. L. Spek, *J. Non-Cryst. Solids*, **176**, 164–171 (1994).
11) K. Matusita and M. Tashiro, *J. Ceram. Soc. Japan*, **81**, 500–506 (1973).
12) K. Engel and G. H. Frischat, *J. Non-Cryst. Solids,* **196**, 339–345 (1996).
13) Y. Iqbal, W. E. Lee, D. Holland and P. F. James, *J. Non-Cryst. Solids*, **224**, 1–16 (1998).
14) L. L. Burgner and M. C. Weinberg, *J. Non-Cryst. Solids*, **279**, 28–43 (2001).
15) V. M. Fokin, E. D. Zanotto and J. W. P. Schmelzer, *J. Non-Cryst. Solids,* **321**, 52–65 (1998).
16) P. C. Soares Jr., E. D. Zanotto, V. M. Fokin and H. Jain, *J. Non-Cryst. Solids*, **331**, 217–227 (2003).
17) V. M. Fokin, M. F. Nascimento and E. D. Zanotto, *J. Non-Cryst. Solids*, **351**, 789–794 (2005).
18) Y. Ding, Y. Miura and H. Yamaji, *Phys. Chem. Glasses*, **39**, 338–343 (1998).
19) Y. Ding, S. Jiang, T. Luo, Y. Hu, Y. Miura and N. Peyghambarian, *Electronics Lett.*, **35**, 504–505 (1999).
20) A. Duran and J. M. F. Navarro, *Phys. Chem. Glasses*, **26**, 126–131 (1985).
21) R. P. S. Chakradhar, B. Yasoda, J. L. Rao and N. O. Gopal, *J. Non-Cryst. Solids*, **352**, 3864–3871 (2006).